JACS
JOURNAL OF THE AMERICAN CHEMICAL SOCIETY

ARTICLE

pubs.acs.org/JACS

A Glimpse at the Chemistry of GeH_2 in Solution. Direct Detection of an Intramolecular Germylene−Alkene π-Complex

Paul S. Billone,[†] Katie Beleznay,[‡] Cameron R. Harrington,[§] Lawrence A. Huck,[∥] and William J. Leigh*

Department of Chemistry and Chemical Biology, McMaster University, 1280 Main Street West, Hamilton, ON Canada L8S 4M1

Supporting Information

ABSTRACT: The photochemistry of 3-methyl-4-phenyl-1-germacyclopent-3-ene (**4**) and a deuterium-labeled derivative (**4**-d_2) has been studied in solution by steady state and laser flash photolysis methods, with the goal of detecting the parent germylene (GeH_2) directly and studying its reactivity in solution. Photolysis of **4** in C_6D_{12} containing acetic acid (AcOH) or methanol (MeOH) affords 2-methyl-3-phenyl-1,3-butadiene (**6**) and the O−H insertion products $ROGeH_3$ (R = Me or Ac) in yields of ca. 60% and 15−30%, respectively, along with numerous minor products which the deuterium-labeling studies suggest are mainly derived from hydrogermylation processes involving GeH_2 and diene **6**. The reaction with AcOH also affords H_2 in ca. 20% yield, while HD is obtained from **4**-d_2 under similar conditions. Photolysis of **4** in THF-d_8 containing AcOH affords $AcOGeH_3$ and **6** exclusively, indicating that the nucleophilic solvent assists the extrusion of GeH_2 from **4** and alters the mechanism of the trapping reaction with AcOH compared to that in cyclohexane. Laser flash photolysis of **4** in hexanes yields a promptly formed transient exhibiting $\lambda_{max} \approx 460$ nm, which decays on the microsecond time scale with the concomitant growth of a second, much longer-lived transient exhibiting $\lambda_{max} \approx 390$ nm. The spectrum and reactivity of the 460 nm species toward various germylene trapping agents are inconsistent with those expected for free GeH_2; rather, the transient is assigned to an intramolecular Ge(II)−alkene π-complex of one of the isomeric substituted hydridogermylenes derived from a solvent-cage reaction between GeH_2 and its diene (**6**) coproduct, formed by addition of HGe−H across one of the C=C bonds. These conclusions are supported by the results of DFT calculations of the thermochemistry associated with π-complexation of GeH_2 with **6** and the formation of the isomeric vinylgermiranes and 1,2-hydrogermylation products. A different species is observed upon laser photolysis of **4** in THF solution and is assigned to the GeH_2−THF complex on the basis of its UV−vis spectrum and rate constants for its reaction with AcOH and AcOD.

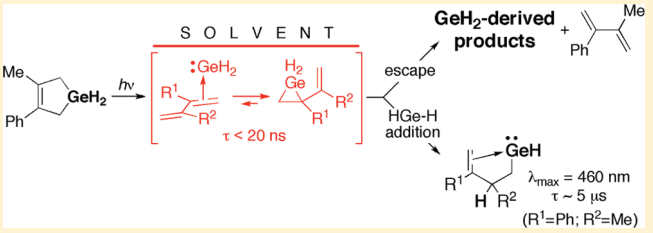

INTRODUCTION

Germylene (GeH_2), the parent Ge^{II} molecule and a key reactive intermediate in the chemical vapor deposition of germane and other germanium hydrides,[1−4] has received considerable attention from spectroscopists, kineticists, and theorists and indeed has been more extensively studied than any other Ge^{II} species, transient or stable.[5,6] Like methylene (CH_2) and silylene (SiH_2), GeH_2 bears the distinction of being the most reactive derivative of its class, according to the extensive kinetic studies that have been carried out on it and other simple germylene derivatives in the gas phase as well as in solid matrixes at very low temperatures.[7] In the gas phase, it reacts with alkenes,[8−11] dienes,[8] alkynes,[8,12−14] hydridosilanes[8,15,16] and -germanes,[17−20] water,[21] and alcohols[21] at rates approaching the collisional limit, generally several orders of magnitude faster than its simplest dialkyl congener, dimethylgermylene ($GeMe_2$).[5,6] Most of these reactions proceed with negative activation energies, which has been rationalized in terms of the initial, reversible formation of a pre-reaction complex in which association of the substrate with GeH_2 occurs via interaction with the empty 4p orbital.[5,6] This process is barrierless for most substrates and at least moderately exothermic, with the rate-limiting barrier for product formation being the one associated with rearrangement of the intermediate complex, via a process that can be thought of most simply as involving attack of the germanium lone pair back into an electrophilic site in the complex.[6] This common pattern of reactivity underlies the recent successful syntheses by Rivard and coworkers of stable donor/acceptor-coordinated complexes of GeH_2.[22] other, similarly-stabilized complexes of transient divalent Group 14 compounds have also been reported recently.[22b,23]

One expected reaction of the species that has not yet been observed is dimerization to form digermene (Ge_2H_4), which theory indicates should be as much as ca. 50 kcal mol^{-1} exothermic.[24−28] Digermene ($H_2Ge{=}GeH_2$) and its various isomers (germylgermylene ($HGeGeH_3$) and the cis and trans hydrogen-bridged GeH_2 dimers ($HGeH_2GeH$)) have been the subject of numerous theoretical studies, which predict the doubly bonded and germylgermylene isomers to be the most stable isomers, approximately isoenergetic,[26,29−32] and separated by a modest (ca. 12 kcal mol^{-1})[29,30] enthalpic barrier. Both digermene[32,33] and germylgermylene[32] have been successfully characterized by infrared spectroscopy in H_2[33] or GeH_4[32]

Received: February 16, 2011
Published: June 03, 2011

matrixes at 8−12 K but to our knowledge have not yet been characterized in the gas phase or in solution.

Recent work from our laboratory has focused on the generation and direct detection of simple transient germylene derivatives such as dimethyl-,[34−38] diphenyl-,[34,36,37,39−41] and methylphenylgermylene[42] ($GeMe_2$, $GePh_2$, and GeMePh, respectively) in solution and on detailing the kinetics and mechanisms of their reactions with various representative germylene substrates. In the case of $GeMe_2$, whose reactivity has been studied both in the gas phase[43] and in hexane solution[35] with a number of common or closely analogous substrates, there is good agreement between the UV−vis spectra and absolute rate constants measured under the two sets of conditions.[6] The main goal of the present work was to see whether we could extend these comparisons to the parent germylene, GeH_2; its UV−vis spectrum in the gas phase, measured by laser-induced fluorescence excitation spectroscopy, is centered at $\lambda_{max} \approx 515$ nm.[44]

Gas-phase kinetic studies of GeH_2 have employed phenylgermane (**1a**), mesitylgermane (**1b**), or 3,4-dimethylgermacyclopent-3-ene (**2**) as photochemical precursors, monitoring the strong rovibrational transitions at 17 111.31 or 17 118.67 cm^{-1} (~588 nm) in the electronic spectrum of the $^{74}GeH_2$ isotopomer for the measurement of decay kinetics, and an ArF excimer laser (193 nm) for precursor excitation.[6,8,9,15,16,18,19,21,45] Phenylgermane (**1a**) has also been shown to extrude GeH_2 upon 248 nm excitation in the gas phase.[18] We have shown that phenylated germacyclopent-3-ene derivatives such as **3a**,**b** are efficient 248 nm precursors for $GeMe_2$ in solution[35] and exhibit sufficiently strong absorptions at 248 nm that it is possible to work with precursor concentrations on the order of 10^{-4} M or less in laser photolysis experiments.[35] It thus seemed reasonable to expect that the dihydro-analogue of **3b**, 3-methyl-4-phenylgermacyclopent-3-ene (**4**), might be a similarly efficient photochemical precursor to GeH_2, thus potentially providing the means to generate the parent germylene in solution under conditions where possible complications due to undesired reactions with its precursor might be minimized. The latter seemed a valid concern since GeH_2 is known to react with hydridogermanes at close to the collisional limit in the gas phase, and the rate varies only modestly with substitution.[17−21,46] The C=C bond in **4** provides a second potential site of undesired precursor reactivity; while less is known in regard to substituent effects on the rate constant than is the case with Ge−H insertions, GeH_2 reacts with both ethene[9] and propene[10] at close to the collisional rate in the gas phase, via a complex series of processes involving (in the case of ethene) both germirane and ethylgermylene as intermediates.[6,9,11] In any event, we expected the styrenyl chromophore in **4** to provide a sufficiently high absorption cross-section at the (248 nm KrF laser) excitation wavelength that precursor concentrations could be kept low and thus minimize complications of this type.

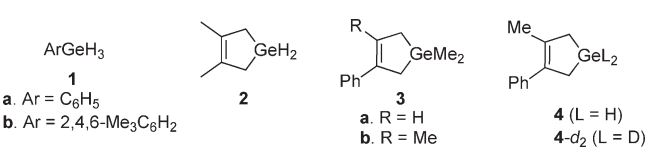

We have thus synthesized **4** and examined its photochemistry in solution by steady state and laser flash photolysis methods. To assist in the identification of GeH_2-derived products in steady state trapping studies, we have also studied the 1,1-dideuterated isotopomer (**4**-d_2). The structural assignments for the primary transient products observed in laser photolysis experiments with **4** and many of our mechanistic conclusions are supported by the results of DFT calculations, which have been carried out at the PW91PW91[47]/6-311+G(2d,p) level of theory.

RESULTS AND DISCUSSION

Compounds **4** and **4**-d_2 were synthesized by reduction of the corresponding dichloride (**5**; eq 1)[35] with $LiAlH_4$ and $LiAlD_4$, respectively, following the procedure reported for the synthesis of **2**.[8]

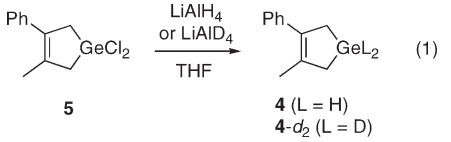

Photochemical Product Studies. Steady state photolysis experiments were carried out in quartz NMR tubes, using deoxygenated solutions of **4** (0.025 M) in cyclohexane-d_{12} or THF-d_8 containing 0.05−0.25 M acetic acid (AcOH), acetic acid-*O*-*d* (AcOD), or methanol (MeOH) as germylene trapping agents. The solutions were irradiated with 254 nm light and were monitored by ^{1}H NMR spectroscopy at selected time intervals between 0 and ca. 40% conversion of **4**. Product yields were determined from the relative slopes of concentration vs time plots covering the range of 0 to 6−10% conversion of **4**. Photolysis of the compound in the absence of a trapping agent afforded only polymeric material, and no small-molecule products of any type could be detected in spite of efficient consumption of the precursor.

Photolysis of **4** in C_6D_{12} containing AcOH or MeOH afforded mixtures of several products in both cases (Figures S1, S2, Supporting Information). The products that could be identified were 2-methyl-3-phenyl-1,3-butadiene (**6**),[35] molecular hydrogen, and the oxygermanes **7** and **8**, respectively (eq 2; Figure S3a, Supporting Information), which were identified by comparison to the reported ^{1}H NMR spectra and the results of deuterium-labeling studies (vide infra).[48,49] The yield of H_2 formed in the presence of AcOH was corrected for the 3:1 ratio of *ortho*-H_2 to *para*-H_2 expected at room temperature (the latter is NMR inactive).[50]

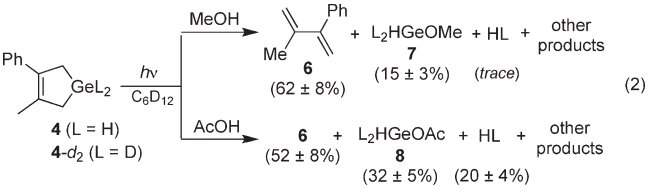

The identities of **8** and H_2 in the photolysis in the presence of AcOH were confirmed by deuterium-labeling experiments, in which **4** and **4**-d_2 were photolyzed in C_6D_{12} containing AcOD and AcOH, respectively, under similar conditions to those used in the experiment with the unlabeled compounds (see Figure 1 and Figures S4, Supporting Information). In both cases, the singlet at δ 4.54 in the ^{1}H NMR spectra of the photolyzed **4**/AcOH mixture was replaced by a 1:1:1 triplet centered at δ 4.51, which could be definitively assigned to HD on the basis of its characteristic coupling constant, J_{HD} = 42.68 Hz.[51] These results indicate that one of the H-atoms in the H_2 that is produced originates from AcOH, while the other originates from **4**, presumably via GeH_2. A second prominent difference

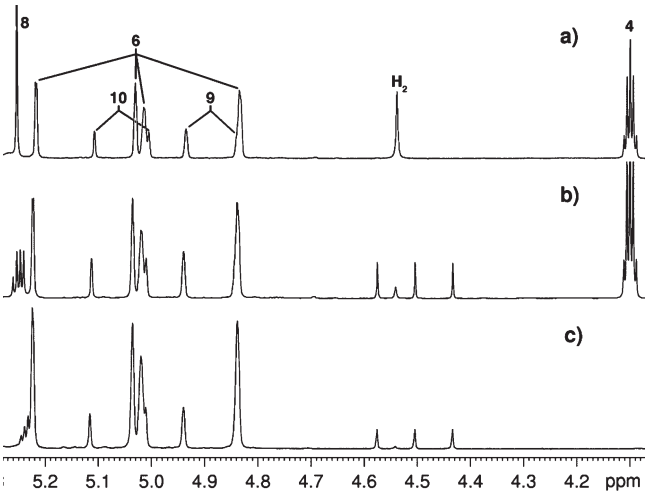

Figure 1. Partial ^{1}H NMR spectra of photolyzed C_6D_{12} solutions of (a) **4** (0.025 M) and AcOH (0.25 M), (b) **4** (0.025 M) and AcOD (0.25 M), and (c) **4**-d_2 (0.025 M) and AcOH (0.25 M).

in these spectra compared to those of the **4**/AcOH photolyzate was the replacement of the singlet at δ 5.26 due to the Ge−H protons in **8** with a 1:1:1 triplet centered at δ 5.24 (J_{HD} = 3.9 Hz) in the case of the **4**/AcOD photolyzate (consistent with $AcOGeH_2D$) and a 1:2:3:2:1 pentet centered at δ 5.23 (J_{HD} = 3.8 Hz) in the case of the **4**-d_2/AcOH photolyzate (consistent with $AcOGeHD_2$).[52] The NMR spectra of a photolyzed mixture of **4**-d_2 and MeOH in C_6D_{12} showed the expected pentet due to the D_2GeH proton in $MeOGeHD_2$ (**7**-d_2).

The NMR spectra also showed resonances throughout the δ 0.5−1.3, δ 2.5−3.5, and δ 5−6 regions of the spectra, none of which were common to both the AcOH and MeOH photolysis mixtures (see Figures S1 and S2, Supporting Information). The spectra of the **4**/AcOH(D) mixtures also contained two additional sets of singlets in the vinylic region which integrated to 28−35% of the areas of the vinylic protons due to **6** (see Figure 1), while the spectrum of the **4**/MeOH mixture contained several singlets in the methoxyl proton region but no new resonances ascribable to vinylic protons. In both cases, several of the multiplets collapsed to lower multiplicities, and some disappeared altogether, in the spectra of the corresponding **4**-d_2/ROH photolysis mixtures (e.g., Figure S4, Supporting Information). GC/MS analysis suggested that these were due to at least three $C_{11}H_{14}Ge$-containing products in both cases; the apparent complexity of the mixtures and the expected delicacy of the compounds[53,54] suggested that isolating them would be quite difficult, so we did not try. Nevertheless, it can be concluded from the deuterium-labeling results that these compounds are formed mainly by hydrogermylation processes, most likely involving the C=C bonds in diene **6**; they are all *primary* reaction products, as they are already present in the mixtures after ca. 1% conversion of **4**. The resolvable spectral features due to two of the minor products formed in the presence of AcOH are consistent with the presence of structures containing the (2-methyl-3-phenyl-3-butenyl)germyl (**9**; δ 1.17 (d), 3.06 (sextet), 5.04 (s), 5.15 (s)) and (3-methyl-2-phenyl-3-butenyl)germyl (**10**; δ 1.56 (s), 3.53 (t), 4.84 (s), 4.93 (s)) functionalities, the allylic hydrogens being the ones originating on germanium. A third type of product (possibly a mix of diastereomers) was formed in significantly higher yield relative to those of **6**, **8**, H_2, and the other minor products when **4** was photolyzed in the presence of a lower (0.05 M) initial concentration of AcOH (Figure S5, Supporting Information). While the deuterium-labeling experiments indicated that it too is derived from a hydrogermylation process, little more structural information than that could be gleaned from the spectra.

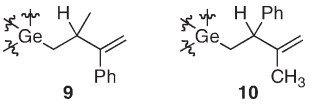

In contrast to the results obtained in C_6D_{12} solution, **6** and **8** were the *only* products detected upon photolysis of a 0.025 M solution of **4** in THF-d_8 containing 0.25 M AcOH (see eq 3 and Figure S6, Supporting Information). Concentration vs time plots showed that the rate of formation of **6** matched that of consumption of **4** almost precisely, indicating a nearly quantitative yield of the diene (Figure S3b, Supporting Information). Very different results were obtained when **4** was photolyzed in THF-d_8 containing 0.25 M MeOH; the solution developed an intense yellow color during the first 5−10% conversion of **4**, which was accompanied by the formation of small amounts of **6**, the appearance of a weak singlet at δ 5.52 (perhaps due to **7**), and broad baseline absorptions in the aliphatic and aromatic regions of the spectrum, indicative of polymerization (eq 3).

The results of these experiments show that the photochemistry of **4** is broadly analogous to that of the methylated derivatives **3a** and **3b**,[35] affording diene **6** as the major product in the presence of MeOH or AcOH and the O−H insertion products expected from reaction of GeH_2 with the hydroxylated substrates; qualitative comparisons of the photolysis efficiencies indicate

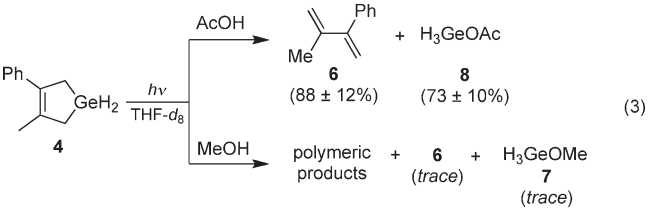

(3)

that the photolysis quantum yield of **4** is similar to those of **3a**,**b** ($\Phi \approx 0.5$[34,35]) as well. However, while photolysis of **3b** affords **6** and $GeMe_2$-derived products in close to quantitative yields,[35] the diene accounts for only 50−60% of the material balance in the photolysis of **4** under similar conditions. This is due to other primary reactions involving Ge−H moieties and suggests the intervention of a reaction intermediate formed competitively with GeH_2 and **6** or prior to it, affording "trappable" GeH_2 in one of two or more competing decomposition channels. These competing reactions are essentially eliminated in THF-d_8, where **6** and **8** are produced almost exclusively. While we cannot rule out the possibility of a solvent effect on the photochemistry of **4** that is not evident with the substituted germacyclopent-3-enes we have studied previously,[34,35] this is consistent with the proposal that the formal extrusion of GeH_2 from **4** proceeds via a short-lived reaction intermediate that possesses more than one pathway for reaction. The additional pathway(s), which the AcOH-trapping results suggest involve addition of Ge−H across the C=C bonds in diene **6**, are presumably suppressed in favor of formal GeH_2 extrusion in the O-donor solvent owing to the latter's ability to stabilize the highly reactive germylene by Lewis acid−base complexation.[36,55] The competing processes are presumably

Scheme 1

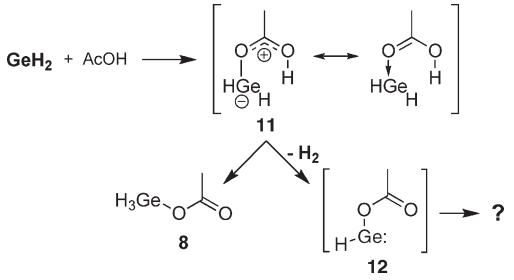

thermally activated, though at this stage we cannot rule out the possibility that they might arise from a secondary photochemical reaction of the putative reaction intermediate, provided its lifetime is sufficiently long to allow its steady state concentration to build up to appreciable levels.

A mechanism to account for the formation of **8** and H_2 from the reaction of GeH_2 with AcOH is shown in Scheme 1 and involves initial Lewis acid−base complexation with the basic site in the substrate[40] followed by competing H-migration from oxygen to germanium (yielding **8**) and H_2 elimination to afford the secondary (acetoxy)germylene **12**. The latter species presumably accounts for some of the unidentified products in the photolyzate. It should be noted that the sum of the yields of **8** and H_2 is roughly equal to that of diene **6**, indicating that the scavenging of GeH_2 by AcOH proceeds essentially quantitatively. A related competition is also evident in the trapping experiment with MeOH, but the reaction affords H_2 in substantially lower yield relative to the insertion product (**7**) than is the case with AcOH. Presumably, this is because in the latter case H_2 elimination from the complex (**11**) proceeds via a six-membered transition state rather than the more restrictive four-membered transition state that is required in the case of the GeH_2−alcohol complex; the higher Brønsted acidity of the carboxylic acid may also contribute to the difference to some extent.[55,56] The competition between insertion and elimination in the reactions of GeH_2 with MeOH has been studied computationally (vide infra),[55,56] but to our knowledge this is the first experimental observation of the H_2-elimination channel in the reaction of hydroxylic substrates with GeH_2.

The relative yields of **6**, H_2, and **7** in the trapping experiments with MeOH indicate the alcohol to be a significantly less efficient trapping agent for GeH_2 than the carboxylic acid, in contrast to the behavior observed by us previously in similar experiments with $GeMe_2$ and $GePh_2$.[34,35] We speculate that this is due to the fact that, as we showed to be the case with the latter derivatives,[34,35] the product-forming steps from the GeH_2−MeOH complex are much slower than is the case with the GeH_2−AcOH complex and thus compete less effectively with dissociation back to the free reactants. The net result is the formation of significant amounts of polymeric material, at the expense of the O−H insertion product **7**. Interestingly, theory predicts that H_2-elimination proceeds via a ca. 6 kcal mol^{-1} lower enthalpic barrier than insertion and should thus dominate the product mixture from decomposition of the GeH_2−MeOH complex.[55,56] Our experimental results indicate that H_2 is in fact formed in only trace amounts in the trapping reaction with the alcohol, in apparent conflict with the theoretical prediction. However, this is most likely because in solution the net insertion process can occur by a catalytic pathway involving a second

Scheme 2

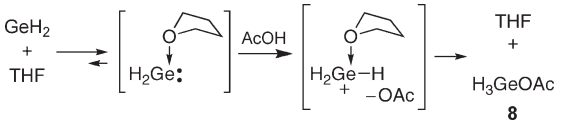

molecule of alcohol as catalyst for H-migration in the complex,[37] which supplants the (higher energy) unimolecular H-migration pathway that was considered computationally.

The complete suppression of the H_2-elimination pathway and the higher material balance in the reaction with AcOH in THF can be explained as being due to the operation of a different mechanism for the reaction of GeH_2 with AcOH in the ether solvent, where GeH_2 is expected to exist as the Lewis acid−base complex with the solvent. As has been shown for $GeMe_2$ and $GePh_2$,[37] complexation of GeH_2 with the ether can be expected to enhance its reactivity toward electrophilic substrates and decrease its reactivity toward nucleophilic ones. We thus envisage the reaction with AcOH in THF as proceeding via initial protonation of the GeH_2−THF complex at germanium, either with concerted displacement of the solvent molecule by the nucleophilic end of the substrate or in stepwise fashion via a (presumably very short-lived) ion pair (see Scheme 2). In any event, the process requires a relatively acidic substrate to be fast, which explains the failure of MeOH to trap the germylene in detectable amounts in this solvent.

Laser Flash Photolysis Studies. Laser flash photolysis of flowed, deoxygenated solutions of **4** ($(5-7) \times 10^{-5}$ M) in anhydrous hexanes, using the pulses from a KrF excimer laser (248 nm, ∼20 ns, ∼100 mJ) for excitation, led to the formation of two distinct transient species with different but clearly related growth/decay behaviors. The shorter-lived of the two species appeared to be formed with the laser pulse, exhibits λ_{max} = 460 nm, and decayed over ca. 20 μs with reasonably clean second-order kinetics. The second species (λ_{max} = 390 nm) grows in after the pulse, reaching a maximum in concentration within ca. 3 μs and then decaying over ca. 100 μs, also with predominant second-order kinetics. The decay rates of both signals increased along with their peak intensities when the excitation laser intensity was increased, as expected for second-order decay processes. Figure 2 shows transient spectra recorded 16−60 ns and 5.5−6.0 μs after the laser pulse, along with representative transient absorption profiles recorded at monitoring wavelengths of 470 and 380 nm; the two species were monitored at wavelengths longer and shorter, respectively, than the absorption maxima to minimize interference from the other species in the kinetic analyses. Analysis of transient absorbance vs time data at the two monitoring wavelengths according to eq 4 afforded second-order decay coefficients of $2k_{dim}/\varepsilon_{470\text{-}nm} = (4 \pm 1) \times 10^7$ cm s^{-1} and $2k_{dim}/\varepsilon_{370\text{-}nm} = (1.4 \pm 0.1) \times 10^6$ cm s^{-1}, respectively.

$$\Delta A_t = \Delta A_0/[1 + (2k_{dim}\Delta A_0/1\varepsilon)t] \quad (4)$$

Addition of acetic acid caused the decay of the 460 nm transient (monitored at 470 nm) to accelerate and follow clean pseudo-first-order kinetics, with little or no change in the initial absorbance of the signal (ΔA_0) compared to that obtained in the absence of added substrate. At the same time, the growth rate of the 390 nm transient was accelerated and its peak intensity was reduced, indicating that its formation is quenched in the presence of the carboxylic acid; this leads to the conclusion that the

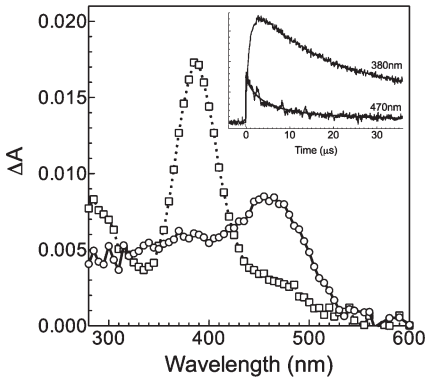

Figure 2. Transient absorption spectra from laser photolysis of **4** in deoxygenated hexane solution at 25 °C, recorded 16−60 ns (-○-) and 5.5−6.0 μs (···□···) after the laser pulse. The inset shows transient growth/decay profiles recorded at 470 and 380 nm. The solid curve drawn through the 470 nm decay is the best fit of the data to eq 4.

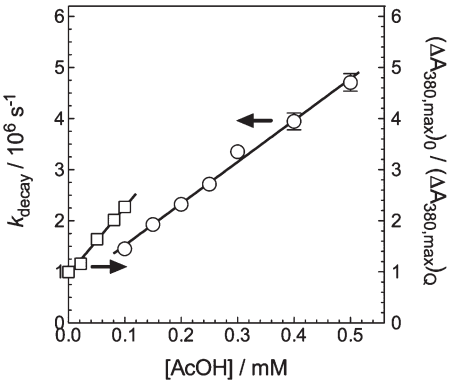

Figure 3. Plots of k_{decay} (○) and $(\Delta A_{380,max})_0/(\Delta A_{380,max})_Q$ (□) vs [AcOH] for the 470 and 380 nm transient signals, respectively, from laser photolysis of **4** in deoxygenated hexanes at 25 °C. The solid lines in (c) are the linear least-squares fits of the data to eqs 5 and 6, respectively.

390 nm transient is a reaction product of the first-formed species. Figure S7 (Supporting Information) illustrates the observed effects on the transient signals as a function of AcOH concentration. Plots of the first-order decay rate coefficient of the 470 nm signal (k_{decay}) vs scavenger concentration ([Q]) were linear and were analyzed according to eq 5, where k_Q is the second-order rate constant for the reaction with the scavenger and k_0 is the (hypothetical) pseudo-first-order decay rate coefficient when [Q] = 0. Linear plots were also obtained from analysis of the relative peak intensities of the 380 nm signal in the absence and presence of the substrate according to eq 6, where $(\Delta A_{380,max})_0$ and $(\Delta A_{380,max})_Q$ are the peak signal intensities in the absence and presence of Q and K_{SV} is a proportionality factor reflecting the efficiency with which the formation of the 390 nm species is quenched by the substrate. Figure 3 shows the plots of k_{decay} and $(\Delta A_{380,max})_0/(\Delta A_{380,max})_Q$ vs [Q] obtained in the experiments. Analysis of the data according to eqs 5 and 6 afforded values of $k_Q = (8.1 \pm 0.6) \times 10^9$ M^{-1} s^{-1} and $K_{SV} = 13\,200 \pm 1400$ M^{-1}, respectively.

$$k_{decay} = k_0 + k_Q[Q] \quad (5)$$

$$(\Delta A_{380,max})_0/(\Delta A_{380,max})_Q = 1 + K_{SV}[Q] \quad (6)$$

The transient spectra of Figure 2, the nature of their temporal evolutions, and the response of the two species to the addition of AcOH are all broadly consistent with a germylene and digermene assignment for the 460 and 390 nm transient products of laser photolysis of **4**, respectively, based on the behavior we have observed previously for substituted germylenes[34−36,39,40,42] and silylenes[57,58] under conditions similar to those employed here. However, there are several discrepancies between the observed results and those expected for GeH_2 and Ge_2H_4 based on previously published experimental and (or) theoretical data for the two species in the gas phase. First, the absorption maxima do not agree well with the values predicted for GeH_2 and Ge_2H_4 by time-dependent DFT calculations (vide infra and ref 34) or with the experimental gas-phase fluorescence excitation spectrum of GeH_2 ($\lambda_{max} \sim 515$ nm).[44] This contrasts the excellent agreement that exists between the gas-phase,[43] solution-phase,[34,35,38] and theoretically predicted[34] UV−vis spectra of $GeMe_2$ ($\lambda_{max} \sim 470$ nm) and the similarly close agreement between the theoretical and experimental (solution-phase) spectra of Ge_2Me_4 ($\lambda_{max} \sim 370$ nm).[34,35,38,59] Second, the rate coefficient for dimerization of the 460 nm transient ($2k_{dim}/\varepsilon_{470\text{-nm}} = (4 \pm 1) \times 10^7$ cm s^{-1}) is substantially lower than would be expected for GeH_2 based on that determined for $GeMe_2$ under similar conditions ($2k_{dim}/\varepsilon_{480\text{-nm}} = (1.5 \pm 0.3) \times 10^8$ cm s^{-1}),[35] assuming the molar extinction coefficient of the GeH_2 absorption is not substantially larger than that of $GeMe_2$ ($\varepsilon_{max} = 750 \pm 300$ dm^3 mol^{-1} cm^{-1}).[35] Third, the rate constant for reaction of the 460 nm species with AcOH is similar to the average of the values reported for $GeMe_2$ under similar conditions ($k_Q = (9.4 \pm 2.0) \times 10^9$ M^{-1} $^{-1}$)[35,38]—not a factor of 2−3 higher (i.e., diffusion-controlled), as might be predicted based on the fact that GeH_2 is characteristically at least 10 times more reactive than $GeMe_2$ toward most common substrates in the gas phase.[6] Finally, the fact that the 460 nm species is nevertheless quenched rapidly and efficiently by AcOH demands that if it were GeH_2 then we should be able to trap it cleanly in steady state photolysis experiments, which is not the case. This all leads us to conclude that the 460 nm species is almost certainly *not* GeH_2, and thus the 390 nm species formed as the primary product of its decay is *not* Ge_2H_4. If free GeH_2 is produced by laser photolysis of **4** under these conditions, then we are unable to detect it.

The kinetic behaviors of the 460 and 390 nm species were also examined in the presence of various other germylene scavengers whose reactivities toward $GeMe_2$ under similar conditions have been quantified.[35] These included triethyl- and *n*-butylamine (Et_3N and *n*-$BuNH_2$, respectively), MeOH, THF, 3,3-dimethyl-1-butyne (TBE), 4,4-dimethyl-1-pentene (DMP), isoprene, triethylsilane (Et_3SiH), and triethylgermane (Et_3GeH). In all cases but MeOH, THF, DMP, and isoprene (vide infra), addition of the substrate caused similar effects on the transient profiles at 470 and 380 nm as were observed with AcOH. The k_Q and K_{SV} values determined in these experiments are listed in Table 1, along with the corresponding values of k_Q for $GeMe_2$ under similar conditions.[35,36]

In the experiments with MeOH and THF in hexanes, addition of the O-donors appeared to cause decreases in the initial signal intensities of the 460 nm species, to an extent that increased with increasing concentration (see Figure S8, Supporting Information). This was accompanied by the appearance of new transient absorptions centered at λ_{max} = 310 and 320 nm, respectively, which are consistent with germylene−O-donor Lewis acid−base complexes; the spectra (Figures S9 and S10, Supporting Information) are both red-shifted relative to those of the

Table 1. Bimolecular Rate and Equilibrium Constants (k_Q and K_{eq}, Respectively) and K_{SV} Values for Quenching of the 460 and 390 nm Transient Products, Respectively, From Laser Photolysis of 4 in Deoxygenated Hexanes Solution at 25 °C by Various Substrates[a]

substrate	$k_Q/10^9$ M^{-1} s^{-1}	K_{SV}/M^{-1}	$k_Q/10^9$ M^{-1} s^{-1} ($GeMe_2$)[b]
Et_3N	5.4 ± 0.5	1500 ± 400	8.7 ± 0.7
n-$BuNH_2$	11.3 ± 0.8	11100 ± 140	12 ± 3
AcOH	8.1 ± 0.6	13200 ± 1400	9.4 ± 2.0[c]
Et_3SiH	0.00013 ± 0.00006	2.8 ± 1.4	0.00055 ± 0.00015
Et_3GeH	0.056 ± 0.005	11 ± 2	0.045 ± 0.015
3,3-dimethyl-1-butyne (TBE)	5.3 ± 0.2	4400 ± 200	11 ± 2[c]
4,4-dimethyl-1-pentene (DMP)	0.072 ± 0.004 (K_{eq} = 45 ± 10 M^{-1})	108 ± 5	9.6 ± 1.2
isoprene	<0.03	–	10.8 ± 2.8
MeOH	(K_{eq} = 280 ± 40 M^{-1})[d]	510 ± 40	(K_{eq} = 900 ± 60 M^{-1})
THF	8.4 ± 1.1 (K_{eq} = 2400 ± 150 M^{-1})	64 ± 1	11 ± 2 (K_{eq} = 9800 ± 3800 M^{-1})

[a] Also listed are the corresponding values of k_Q and (or) K_{eq} for quenching of $GeMe_2$ by the same substrates under similar conditions.[35,36]. [b] Data from refs 35, 36, and 38. [c] Average of 2−3 independent determinations using different precursors. [d] k_Q is too fast to measure, given the magnitude of K_{eq}.

corresponding $GeMe_2$−O-donor complexes under similar conditions.[36] The effects on the intensities and decay kinetics of the 460 nm species are again quite similar to those observed previously for $GeMe_2$ in the presence of low concentrations of THF and MeOH in hexanes[36] and are consistent with reversible reaction with the O-donor substrates. With THF, the equilibrium constant is of an appropriate magnitude for both the approach to equilibrium and the residual amount of the free species present at equilibrium to be detected, while with MeOH the behavior is consistent with a rapidly attained but relatively unfavorable reversible process for which only the residual amount of free 460 nm species present at equilibrium can be detected.[36] Analysis of the data in the manner detailed in our earlier study of $GeMe_2$[36] affords the forward rate and equilibrium constants listed in Table 1 (see Figures S11 and S12, Supporting Information). The k_Q^{THF} value is again similar to that for the corresponding reaction with $GeMe_2$, while the equilibrium constants are both 3−4 times smaller than the $GeMe_2$ values.[36]

Unusually,[35,39,42] addition of 0.5−2.0 mM isoprene or DMP had *no* discernible effect on the intensity or decay characteristics of the 460 nm species and caused only a marked lengthening in the growth time of the 380 nm signal and slight increases in its maximum intensity. The behavior of the 380 nm signal suggests that the substrate acts to slow down the reaction channel which leads to the formation of the 390 nm transient product. Addition of larger quantities (10−80 mM) of the alkene caused similar effects on the 470 nm signals as were observed in the experiments with THF, and similar analyses of the data afforded rate and equilbrium constants of k_Q = (7.2 ± 0.4) × 10^7 M^{-1} s^{-1} and K_{eq}^{DMP} = 45 ± 10 M^{-1}, respectively, for reaction of the species with DMP. The rate constant is ca. 100 times smaller, and the equilibrium constant at least 500 times smaller, than those for reaction of $GeMe_2$ with the same substrate under similar conditions.[35]

Laser photolysis of **4**-d_2 in anhydrous hexanes resulted in transient spectroscopic behavior very similar to that obtained in the experiments with **4** under similar conditions (see Figure S13, Supporting Information), but with one important difference. In this case, the rising edge of the 470 nm absorption exhibited a slight growth that could not be detected in the experiments with the protiated derivative, suggesting that the rate of formation of the species is subject to a kinetic isotope effect.

Transient decays recorded for deoxygenated solutions of **4** in neat THF afforded bimodal decays in the 280−330 nm range, consisting of a short-lived component ($\tau \sim 5\ \mu s$; $\lambda_{max} \sim 310$ nm) superimposed on a long-lived signal ($\tau \sim 150\ \mu s$; $\lambda_{max} \sim 290$ nm) that decayed to a stable residual absorption with $\lambda_{max} < 280$ nm. Saturation of the solution with air rendered the short-lived component unresolvable from the laser pulse and afforded a single transient species which exhibited an apparent absorption maximum at λ_{max} = 290 nm and decayed with complex kinetics, as shown in Figure 4a. Addition of AcOH or AcOD to the air-saturated solution led to a shortening of the lifetime of the 290 nm species in proportion to concentration, and plots of k_{decay} vs [AcOL] (L = H or D) according to eq 5 were linear (see Figure 4b), affording rate constants of k_{AcOH} = (2.5 ± 0.2) × 10^5 M^{-1} s^{-1} and k_{AcOD} = (1.0 ± 0.2) × 10^5 M^{-1} s^{-1} (k_H/k_D = 2.5 ± 0.7). These values are both ca. 50 times smaller than those reported by us previously for the corresponding reactions of the $GeMe_2$−THF complex in THF solution.[37]

The transient behavior in the presence of MeOH and THF in dilute hexanes and in the neat O-donors is consistent with an assignment of the 310−320 nm species to germylene−MeOH and germylene−THF complexes, respectively, though it is quite likely that the species observed in dilute hexanes containing millimolar concentrations of the O-donors are different than those observed in the neat liquids. This conclusion is based on the fact that the differences in the spectra of the two O-donor complexes in dilute hexanes compared to the neat liquids are significantly greater than those exhibited by the $GeMe_2$−MeOH and $GeMe_2$−THF complexes under the two sets of conditions.[37] Since the product studies indicate the chemistry is profoundly cleaner in THF than in hydrocarbon solvents, we assign the transient observed in THF solution to the GeH_2−THF complex. The observation of quenching of the species by AcOH and AcOD, which exhibits a clearly primary kinetic isotope effect, is consistent with this assignment and with the reaction mechanism proposed in Scheme 2. Its lack of reactivity toward MeOH, which the product studies show to be an ineffective scavenger in THF solution, is also consistent with the assignment. We tentatively assign the species observed in neat MeOH solution to the GeH_2−MeOH complex.

Comparison of the rate and equilibrium constants for reaction of the 460 nm species with the corresponding ones for $GeMe_2$

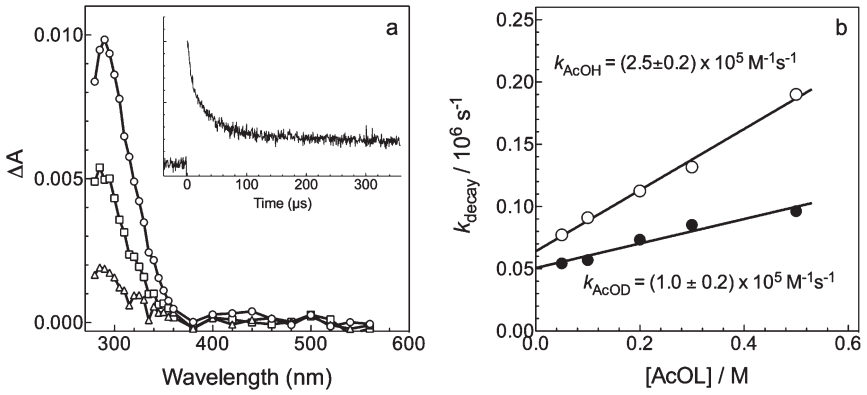

Figure 4. (a) Transient absorption spectra of a 0.14 mM solution of **4** in air-saturated THF, 0−1.3 μs (-○-), 19.8−22.4 μs (-□-), and 343−347 μs (-Δ-) after the laser pulse; the inset shows a transient decay profile recorded at 290 nm. (b) Plots of k_{decay} vs [AcOL] (L = H or D) for quenching of the 290 nm species by AcOH and AcOD in air-saturated hexane at 25 °C.

under similar conditions (Table 1) confirms our initial conclusion that the spectroscopic and kinetic behavior exhibited by the species is inconsistent with what is expected for free GeH_2. The 460 nm transient reacts with amines, AcOH, Et_3SiH, Et_3GeH, TBE, DMP, isoprene, and THF with rate constants that are in almost every case smaller than the corresponding values for $GeMe_2$,[35,36] in some cases by a sizable margin. Rate constants have been reported for reaction of GeH_2 in the gas phase with the same or similar substrates, and they are in every case significantly greater than those exhibited by $GeMe_2$ under the same conditions.[6,8−10,13−15,19,20,43] Nevertheless, the species exhibits all of the characteristics expected for a germylene derivative, with the exception of its anomalously low reactivity toward isoprene and DMP. The behavior seems more compatible with a germylene−alkene π-complex than a free germylene.

The occurrence of competing solvent cage reactions between GeH_2 and its diene (**6**) coproduct provides a reasonable explanation for the results of both the steady state and laser photolysis experiments with **4** and **4**-d_2; our proposed mechanism (Scheme 3) draws on the gas-phase kinetics and computational studies of the reaction of GeH_2 with ethene[9,11] and on the results of recent experimental and computational studies of the reactions of substituted germylenes with conjugated dienes.[35,41,60] The competing reactions in question are (1 + 2)-cycloaddition to the corresponding vinylgermirane (**14**), which is expected to be reversible,[35,41,60] and 1,2-hydrogermylation to afford the corresponding hydridogermylenes **15** or **16**. Each of these processes is expected to involve the prior formation of a π-complex (**13**) between GeH_2 and one of the C=C bonds in the diene.[9,11,35,41,60] Four isomeric hydridogermylenes are possible depending on the preferred regiochemistry of the reaction in the case of the unsymmetrical diene (**6**), two arising from attachment of germanium to one of the terminal carbons of the diene (**15**) and two from attachment to one of the internal carbons (**16**). The NMR characteristics exhibited by two of the minor products formed in C_6D_{12} in the presence of AcOH are consistent with the substituted 3-butenyl side chain present in **15**. Furthermore, the conformational flexibility afforded by the two-carbon chain separating the Ge(II) center from the terminal C=C bond in the structure should allow the formation of a relatively unstrained intramolecular π-complex (**15-π**), which should exhibit a UV−vis absorption maximum at shorter wavelengths than that of the uncomplexed species and exhibit somewhat different patterns of

Scheme 3

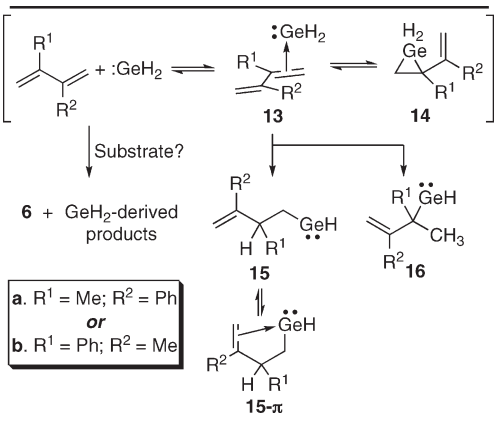

reactivity toward added substrates—alkenes and dienes in particular. The (1 + 2)-cycloaddition process can be viewed as effectively retarding the escape of free GeH_2 and **6** from the solvent cage in which they are formed, allowing the 1,2-hydrogermylation process(es) to compete with cage escape. In THF solution, the solvent cage is itself reactive toward GeH_2 and thus quenches the hydrogermylation process(es) altogether.

The isomeric vinylgermiranes (**14**) can be ruled out as candidates for the 460 nm transient, as they should absorb below 300 nm regardless of the regiochemistry[39] and should also be much less reactive toward the nucleophilic substrates of Table 1 than the measured rate constants indicate. A GeH_2−diene π-complex (e.g., **13**) can also be ruled out, based mainly on the observation of the slight growth in the 460 nm signal obtained with **4**-d_2, which is indicative of a primary isotope effect on the rate of its formation. Furthermore, it is difficult to rationalize the apparent concentration dependence of the product mixture obtained in the presence of 0.05−0.25 M AcOH in the context of an assignment of **13** for the 460 nm species, as it is quenched by this substrate at close to the diffusion-controlled rate; taken together, these two sets of results suggest that the 460 nm species is something that may be formed competitively with GeH_2 or its trapping products but is not itself capable of contributing to their formation. In other words, the 460 nm species is more likely to be

Table 2. PW91PW91/6-311+G(2d,p) and PBE0/cc-pVTZ (in Parentheses) Electronic Energies, Enthalpies (298.15 K), and Free Energies (298.15 K) of Stationary Points in the Reactions of GeH_2 with *s*-trans 2-Methyl-6-phenyl-1,3-butadiene (6) in kcal mol^{-1} Relative to the Isolated Reactants and Predicted UV−vis Absorption Maxima, Calculated for the PW91 Structures at the TDPW91PW91/6-311+G(2d,p), TDPBE0/cc-pVTZ, and TDB2PLYP/6-311G(d,p) Levels of Theory

species	ΔE_{elec}	ΔH_{298K}	ΔG_{298K}	λ_{max} (nm; TDDFT) PW91 | PBE0 | B2PLYP
13a$_{out}$	−23.7 (−21.0)	−21.4 (−18.8)	−9.9 (−7.3)	383 | 361 | 351
$T_{14a,out}$	−19.5	−17.9	−5.3	
14a	−21.2 (−23.1)	−19.1 (−21.0)	−7.4 (−9.1)	284 | 248 | 234
T_{15a}	−16.0 (−14.3)	−14.9 (−13.1)	−2.9 (−1.1)	
15a	−22.3 (−23.9)	−18.6 (−20.1)	−8.7 (−10.0)	535 | 513 | 505
$T_{15a<>15a\text{-}\pi}$	−19.9	−16.8	−5.1	
15a-*π*	−37.4 (−37.7)	−32.9 (−33.1)	−20.4 (−20.5)	462 | 422 | 392
13a$_{in}$	−19.0 (−17.3)	−17.1 (−15.3)	−5.9 (−4.2)	
$T_{14a,in}$	−17.7	−16.3	−4.2	
T_{16a}	−13.4 (−11.3)	−12.1 (−10.0)	−0.1 (+2.2)	
17a-*π*	−36.4 (−36.7)	−32.1 (−32.3)	−20.7 (−20.7)	304 | 276 | 263
13b$_{out}$	−23.5	−21.3	−10.0	419 | 390 | 374
$T_{14b,out}$	−19.4	−17.8	−5.2	
14b	−21.8	−19.9	−8.1	299 | 265 | 247
T_{15b}	−16.3	−15.2	−2.6	
15b	−25.8	−21.9	−10.5	483 | 433 | 399
$T_{15b<>15b\text{-}\pi}$	−20.5	−17.4	−5.6	
15b-*π*	−35.3	−31.0	−20.0	399 | 362 | 335
13b$_{in}$	−18.9	−17.0	−5.5	
T_{16b}	−13.2	−12.1	+0.1	
17b-*π*	−37.4	−33.0	−21.6	322 | 290 | 275

the species responsible for formation of some of the *minor* products observed in the trapping experiments than the major ones.

A hydridogermylene assignment is consistent with this last conclusion, as well as with the apparent isotope effect on the rate of its formation and its generally comparable reactivity toward many of the substrates listed in Table 1 to those reported previously for $GeMe_2$ and $GePh_2$. Intramolecular complexation with the C═C bond at the end of the side chain could explain the unusually low reactivity of the species toward isoprene and the alkene (DMP), as it should reduce the driving force for reaction with the C═C bond(s) of olefinic substrates but may have relatively small effects on the rates of other typical germylene reactions. The C═C bonds in germylenes **15** and (or) **16** may get involved along with the Ge(II) center in reactions with hydroxylic substrates,[61] which could explain why olefinic side products are formed in the reaction with AcOH but are not in that with MeOH (vide supra). If all this is correct, then it is the identities of these minor products that hold the key to the identification of the transient and the mechanism for its formation. With some tentative partial structural information in hand, we turned to computational methods, to see whether they might allow a more definitive structural assignment for the 460 nm transient to be made.

Computational Studies. A portion of the pe surface for the reactions of GeH_2 with diene **6** was explored with density functional methods, carried out at the PW91PW91[47]/6-311+G(2d,p) level of theory. Geometry optimizations and frequencies calculations were carried out for GeH_2 and the *s*-trans conformer of **6**, the four possible *π*-complexes of GeH_2 with the C═C bonds in (*s*-trans) **6** (**13**), the two isomeric vinylgermiranes (**14**) derived from (1 + 2)-cycloaddition, the four possible 1,2-hydrogermylation products (**15** and **16**) and their intramolecular *π*-complexes (**15-*π*** and **17-*π***), and the transition states for formation of **14**−**16** from the corresponding GeH_2−**6** complexes (eq 7). The transition states were confirmed to be first-order saddle points on the basis of their vibrational frequencies, and their connections to reactants and products were established by internal reaction coordinate (IRC) calculations. Figure 5 shows the various structures located in the calculations for the reactions of GeH_2 with the C^1═C^2 bond in *s*-trans **6**, along with selected geometrical parameters. The structures of the corresponding stationary points in the reaction paths involving the C^3═C^4 bond are all quite similar to those involving the other and are shown in the Supporting Information (Figure S14). The bond distances and angles associated with the various structures compare well (where applicable) with those reported previously for the GeH_2 + ethylene[9,62−65] and $GeMe_2$ + 1,3-butadiene[60] systems using other DFT or ab initio methods.

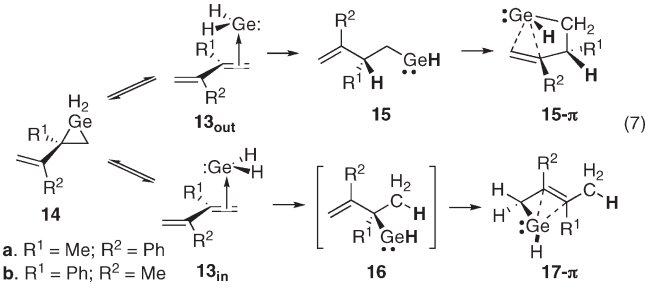

(7)

Interestingly, we were unable to locate an energy minimum corresponding to either isomer of germylene **16**. An IRC calculation confirmed that they are the incipient reaction

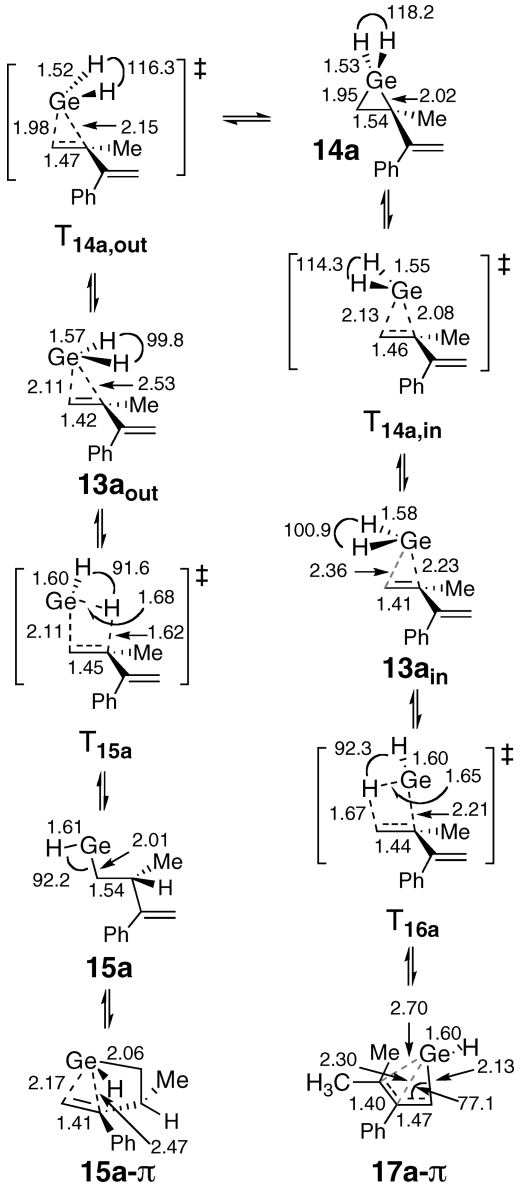

Figure 5. Stationary points and selected geometric parameters on the potential energy surface for reaction of GeH_2 with the $C^1{=}C^2$ bond of 2-methyl-3-phenyl-1,3-butadiene (**6**), calculated at the PW91PW91/6-311+G(2d,p) level of theory.

products from the appropriate transition states (T_{16}), but attempts to optimize their geometries always resulted in rearrangement to **17-π**, the intramolecular π-complexes of the corresponding 1-(*trans*-2-butenyl)germylene derivatives. Thus, the alternate hydrogermylation pathway can be viewed formally as a sequential 1,2-hydrogermylation/[1,3]-GeH migration, the second stage of which proceeds only as far as **17-π**. The migration process is presumably facilitated by the particularly weak bond between Ge and the secondary allylic carbon in the incipient product (**16**). We note that a stable bisgermylene derivative featuring bonding characteristics analogous to that in **17-π** has recently been reported by Power and co-workers.[66]

The calculated thermochemical data for the various structures investigated are listed in Table 2, while Figure 6 summarizes the computed standard free energy surfaces, relative to free GeH_2 and

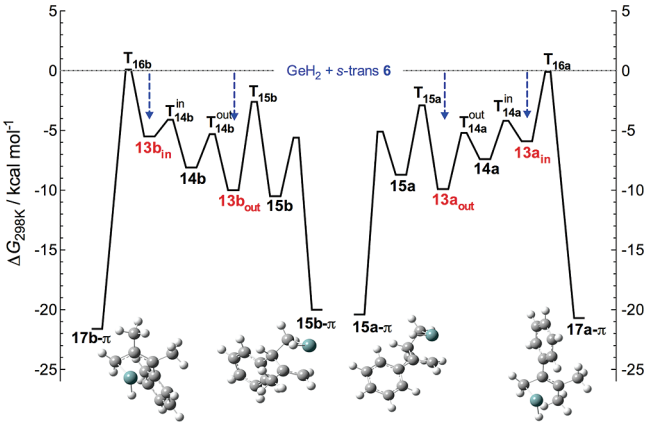

Figure 6. Partial free energy surface for the reactions of GeH_2 with 2-methyl-3-phenyl-1,3-butadiene (**6**), calculated at the PW91PW91/6-311+G(2d,p) level of theory.

s-trans **6**; vibrational frequencies were not scaled. The enthalpy surfaces are shown in Figure S15 (Supporting Information), along with full details of the computed structures. The transition states reported for the conformational interconversion of **15** and **15-π** should be considered somewhat ill-defined, as these processes involve rotations about several single bonds in the structures. The structures reported (see Supporting Information) correspond to eclipsed conformers about the $C^1{-}C^2$ bonds in **15a**,**b**, and while they are true transition states according to the calculations, we could not confirm that they are the actual ones accessed in these processes.

The PW91 method was chosen on the basis of the results of preliminary calculations of three stationary points on the pe surface for the (1 + 2)-cycloaddition of $GeMe_2$ and *s*-trans 1,3-butadiene, which has been characterized previously at the CCSD(T)/cc-pVTZ//B3LYP/6-311G(d,p) level of theory.[60] Our calculations focused on the $GeMe_2$–butadiene π-complex (**18**), the corresponding vinylgermirane (**19**), and the transition state linking them (T_{19}; eq 8) and were also carried out at the B2PLYP[67]/6-311G(d,p), PBE0[68]/cc-pVTZ, and Gaussian-4 (G4)[69] levels; the results are compiled in Table S1 of the Supporting Information. The experimental upper limit of $\Delta G^\circ \leq -4.1$ kcal mol^{-1} for the (1 + 2)-cycloaddition of $GeMe_2$ to isoprene, calculated from the reported lower limit of the equilibrium constant in hexanes solution at 298 K,[35] served as the primary benchmark for the calculations. PW91 and PBE0 both afford overall reaction energies that are consistent with the experimental data for the $GeMe_2$ + isoprene system, as do also the higher level G4 and CCSD(T) methods.

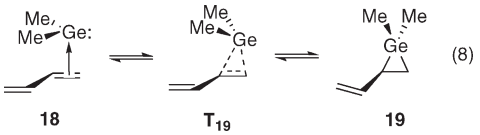

(8)

We could not locate a minimum energy structure for complex **18** or a transition state for the formation of **19** using the PBE0 method, which would seem to indicate it is more reluctant than PW91 to stabilize π-complexes; Birukov et al. experienced similar difficulties with the PBE density functional in their study of the cycloaddition of $GeMe_2$ with ethylene.[64] A similar characteristic appears to be shared as well by the higher level methods, so we also carried out a more limited series of geometry and frequencies calculations on the

GeH_2 + **6** system at the PBE0/cc-pVTZ level, confining our attention to the minima on the C^1-C^2 ("a") half of the pe surface and the transition states T_{15a} and T_{16a}. The calculated energies are included in Table 2; the structures varied only modestly from those obtained at the PW91 level. The PBE0 method predicts a reversal of the relative energies of the vinylgermirane (**14a**) and the "out" π-complex ($\mathbf{13a}_{out}$) compared to PW91. However, the two methods arrive at similar energies for the respective favored structures and similar energies for the hydrogermylation products (**15a**, **15a-π**, and **17a-π**) *and* the transition states leading to them (T_{15a} and T_{16a}).

The energies and oscillator strengths of the six lowest transitions in the electronic spectra of $\mathbf{13}_{out}$, **14**, **15**, **15-π**, and **17-π** were calculated for the PW91PW91/6-311+G(2d,p) structures using time-dependent (TD) DFT at the PW91PW91/6-311+G(2d,p), B2PLYP/6-311G(d,p), and PBE0/cc-pVTZ levels of theory. The predicted longest-wavelength UV−vis absorption maxima obtained from the resulting simulated spectra are listed in Table 2. The spread in the predicted λ_{max} values varies between 0.3 and 0.6 eV for most of the structures investigated, with TDB2PLYP consistently predicting the highest energy value and TDPW91 the lowest.

The same three TDDFT methods were also employed to calculate UV−vis spectra for GeH_2, GeMeH,[70] $GeMe_2$, and the MeOH and THF complexes of GeH_2 and $GeMe_2$ (Table S2, Supporting Information), again employing structures optimized at the PW91 level. The predictions afforded by the three methods for the germylenes agree with the experimental spectra to within 0.13 eV in all cases. For the complexes, the predicted spectra vary with the TDDFT method in a similar way as those for the GeH_2/**6**-derived species, and only TDB2PLYP came reasonably close to reproducing the known experimental spectra of the $GeMe_2$−MeOH and −THF complexes; it incorrectly predicted the former to show the longer-wavelength absorption, however.[36] Similar spectra were predicted for the corresponding GeH_2-derived species.

The calculations confirm that complexation of GeH_2 with one or the other of the C═C bonds in **6** is at least moderately exergonic and that the four possible π-complexes are the critical intermediates in both the (1 + 2)-cycloaddition and hydrogermylation processes; their formation from the isolated reactants is expected to be barrierless.[9,60,62−65] The so-called "out" complexes, in which the lone pair on germanium is pointed along the C═C bond axis away from the bulk of the π-electron density in the diene, are predicted to be 3−5 kcal mol^{-1} lower in energy than the corresponding "in" complexes, presumably because electron−electron repulsion is minimized in the out orientation. The lowest-energy transition state available to both the in and out complexes is that for ring closure to the corresponding vinylgermirane, thus providing a low energy pathway for their interconversion. In any event, the calculations predict that GeH_2 and **6** initially drop into two energy wells, each populated by the in and out complexes and the corresponding vinylgermirane, which define the starting points for further reaction. The calculated barriers for the interconversion of these species are such that equilibrium between $\mathbf{13}_{out}$ and **14** should be established on a time scale of a few nanoseconds or less.

The starting wells are flanked on either side by the transition states for the two hydrogermylation processes (T_{15} and T_{16}), of which that for the formation of **15** (T_{15}), is predicted to be lower by ca. 3 kcal mol^{-1}. Thus, the calculated barriers to reaction at the two individual C═C bonds in the diene predict a clear preference for one hydrogermylation pathway over the other in both cases. Interestingly, however, the two (**a** and **b**) pe surfaces are nearly mirror images of one another, so the calculations further predict that reaction at the two C═C bonds in the diene should occur with minimal regioselectivity. The energy of **15** in its initial geometry is quite similar to that of the minimum in the starting well, but formation of the corresponding intramolecular π-complex (**15-π**) takes it further down in energy by 7−8 kcal mol^{-1}. It is difficult to quantify the free energy barriers for this latter process because of the complexity of the conformational motions that are involved, but it seems safe to assume that they are significantly smaller than those for the return of **15** to the starting wells. In any event, the free energy of activation for the return of **15-π** to **15** is predicted to be at least 12 kcal mol^{-1}, corresponding to a unimolecular rate constant on the order of ca. 10^4 s^{-1} or less. This suggests that the formation of **15-π** should be effectively irreversible on the microsecond time scale under ambient conditions in solution. Provided that further unimolecular reactions of the species are relatively slow, the end result in the absence of a reactive substrate should be dimerization.

The calculations thus point to **15a-π** and **15b-π** as the most likely candidates for the 460 nm transient observed in the laser photolysis experiments with **4**, as we concluded from the experimental results discussed above. The calculated free energies of activation for their formation from the starting wells are on the order of 7−8 kcal mol^{-1} at the present levels of theory, which corresponds to a unimolecular rate constant in the range of ca. $1-5 \times 10^7$ s^{-1}. This is in quite reasonable agreement with the lower limit of ca. 10^8 s^{-1} that is defined by the 20 ns duration of our laser pulse and the fact that the formation of the 460 nm transient from **4** appears to be complete by the end of that time window.

Despite the rather large variation in λ_{max} that the three TDDFT methods predict (Table 2), they all agree that **15a-π** should absorb at significantly lower energies (by 0.5−0.6 eV) than **15b-π**, presumably owing primarily to the difference in the substituents at the C═C bond in the two derivatives: phenyl in the case of **15a-π** vs methyl in **15b-π**. This points to **15a-π** as the more likely assignment for the 460 nm transient. The only other structures that the TDDFT calculations suggest should be considered are the open-chain conformers **15a** and **15b**, but (as discussed above) the calculated energetics and experimental kinetic data dictate against either of these assignments. It is interesting to note that the predicted spectrum of **15b** is blue-shifted somewhat relative to that of **15a**, which may be due to a weak complexing interaction between the Ge(II) center and the phenyl ring two carbons away. Indeed, the calculations suggest **15b** is ca. 2 kcal mol^{-1} more stable than **15a**, presumably for this reason.

If **15b-π** is formed competitively with **15a-π** as the product studies with AcOH suggest, then its absorptions are predicted to lie underneath the strong absorptions in the 360−400 nm region of the spectrum, which are mainly due to the much longer-lived product of dimerization of the 460 nm species. Indeed, the 16−60 ns spectrum of Figure 2 suggests there may be a promptly formed component of the transient absorptions in this range, its maximum blue-shifted slightly relative to the absorption maximum of the long-lived dimeric product. It is difficult to be certain of this, however. The dominant transient absorption in this range exhibits λ_{max} = 390 nm, grows in concomitantly with the decay of the absorptions due to **15a-π**, and then decays over an extended time scale with second-order kinetics, consistent with a digermene assignment. On the basis of the above, we speculate that the

390 nm absorptions are due to a mixture of isomeric digermene dimers of germylenes **15a** and **15b**.

The usual ultimate course of the reactions of germylenes with conjugated dienes is (1 + 4)-cycloaddition via the *s*-cis conformer of the diene, to yield the corresponding germacyclopent-3-ene derivative.[60,71] We have not explored the pe surfaces associated with the *s*-cis conformer of **6**; they can be expected to link to **4** via higher energy transition states than those for the formation of **15** and perhaps **17**-π as well. The (1 + 4)-cycloaddition process could well compete with the hydrogermylation chemistry exhibited by GeH_2 and **6**, but if it does it regenerates **4** and thus constitutes only a source of inefficiency in the formation of products (stable or transient) from the photolysis of **4**. The *actual* competition between these two processes in the reaction of GeH_2 with conjugated dienes distinct from **6** is the subject of continued study in our laboratory.

SUMMARY AND CONCLUSIONS

The results of this work show that 3-methyl-4-phenylgermacyclopent-3-ene (**4**) is a reasonably efficient photochemical precursor to GeH_2 in solution. However, unlike the 1,1-disubstituted derivatives that have been studied previously, photolysis of the compound produces the germylene cleanly only when the solvent is sufficiently nucleophilic to pull the highly reactive parent species out of the solvent cage in which it is formed and away from its coproduct, 2-methyl-3-phenyl-1,3-butadiene (**6**), with which it appears to react at rates similar to or faster than that of diffusional separation in nonviscous hydrocarbon solvents. Thus, in THF solution, photolysis of **4** produces GeH_2 essentially exclusively, in the form of its Lewis acid−base complex with the solvent. Under these conditions, the species can be trapped as the corresponding O−H insertion product by reasonably acidic substrates such as acetic acid. The GeH_2−THF complex has been detected by laser photolysis of **4** in THF solution, and preliminary aspects of its kinetic behavior and reactivity have been determined.

Much more complicated chemistry results from photolysis of **4** in hydrocarbon solvents. Product studies show that diene **6** is formed in only 50−60% yield, along with H_2 and the O−H insertion products expected from reaction of GeH_2 with AcOH and MeOH. Several other products are also formed in both cases; while they have not been fully identified, their NMR characteristics and deuterium-labeling studies clearly show them to be derived from hydrogermylation processes, formally involving a C═C bond in the diene coproduct, GeH_2, and the trapping agent.

Laser photolysis of **4** in hexanes affords a promptly formed transient that exhibits spectral and kinetic characteristics which are more or less typical of reactive germylenes in solution but inconsistent with what would be expected for GeH_2. The species reacts unusually slugglishly (and reversibly) with a terminal alkene and shows no indication of a reaction with isoprene, another normally rapid and efficient scavenger of transient germylenes in solution. It is formed within the ca. 20 ns duration of the laser pulse, but this is slowed detectably in the deuterated analogue of the precursor, indicating a primary isotope effect on the rate of its formation.

The experimental data are accommodated by a mechanism in which GeH_2 and **6** undergo a rapid series of reactions in the solvent cage in which they are formed, which compete with diffusional separation. These are proposed to begin with the spontaneous formation of the various possible π-complexes between GeH_2 and a C═C bond in the diene coproduct. The complexes undergo rapid, competing cyclization to the corresponding vinylgermiranes, which is reversible, and (1,2)-hydrogermylation to yield a mixture of two isomeric 3-butenylhydridogermylene derivatives, which is not. The latter products are then further stabilized by the formation of the corresponding intramolecular Ge(II)−alkene π-complexes. It is these species that are proposed to be mainly responsible for the complicated mixture of minor products observed in steady state trapping experiments and for the 460 nm transient absorption observed in laser photolysis experiments with **4** in hexanes. DFT calculations are in full support of this mechanistic analysis and further support a unique structural assignment for the 460 nm transient product to one of the two possible germylene−alkene π-complexes. The species reacts unusually slowly with alkenes and dienes, partly because the first steps in these reactions involve a similar interaction (i.e., π-complexation) to the intramolecular one that is already present in the molecule and also because the stabilization imparted on the Ge(II) center by complexation reduces the overall driving force for the reactions.

Further studies of the chemistry of the parent Ge(II) derivative in solution and of the scope of intramolecular π-complexation phenomena in germylene (and silylene) chemistry are in progress.

ASSOCIATED CONTENT

Supporting Information. Details of the synthesis and characterization of **4** and **4**-d_2; NMR spectra and concentration vs time plots from steady state photolysis experiments; additional kinetic data determined in laser flash photolysis experiments; details of the computational studies; and tables of calculated Cartesian coordinates and energies. This material is available free of charge via the Internet at http://pubs.acs.org.

AUTHOR INFORMATION

Corresponding Author

leigh@mcmaster.ca

Present Addresses

[†]Department of Chemistry, University of Ottawa, 10 Marie Curie, Ottawa ON Canada K1N 6N5.

[‡]Department of Dermatology and Skin Science, Vancouver General Hospital, 835 West 10th Avenue, Vancouver BC Canada V5Z 4E8.

[§]Syngenta Crop Protection Canada, Inc., 140 Research Lane, Research Park, Guelph, ON Canada N1G 4Z3.

[∥]Department of Chemistry, University of Alberta, 11227 Saskatchewan Drive, Edmonton AB Canada T6G 2G2.

ACKNOWLEDGMENT

We thank the Natural Sciences and Engineering Research Council of Canada for financial support, the McMaster Regional Centre for Mass Spectrometry for mass spectrometric analyses, and Teck-Cominco Metals Ltd. for a generous gift of germanium tetrachloride. Part of this work was made possible by the facilities of the Shared Hierarchical Academic Research Computing Network (SHARCNET:www.sharcnet.ca) and Compute/Calcul Canada.

REFERENCES

(1) Newman, C. G.; Dzarnoski, J.; Ring, M. A.; O'Neal, H. E. *Int. J. Chem. Kinet.* **1980**, *12*, 661.

(2) Dzarnoski, J.; O'Neal, H. E.; Ring, M. A. *J. Am. Chem. Soc.* **1981**, *103*, 5740.
(3) Isobe, C.; Cho, H.-C.; Crowell, J. E. *Surf. Sci.* **1993**, *295*, 117.
(4) Du, W.; Keeling, L. A.; Greenlief, C. M. *J. Vac. Sci. Technol. A* **1994**, *12*, 2281.
(5) Boganov, S. E.; Egorov, M. P.; Faustov, V. I.; Krylova, I. V.; Nefedov, O. M.; Becerra, R.; Walsh, R. *Russ. Chem. Bull. Int. Ed.* **2005**, *54*, 483.
(6) Becerra, R.; Walsh, R. *Phys. Chem. Chem. Phys.* **2007**, *9*, 2817.
(7) Boganov, S. E.; Egorov, M. P.; Faustov, V. I.; Nefedov, O. M. In *The chemistry of organic germanium, tin and lead compounds*; Rappoport, Z., Ed.; John Wiley and Sons: New York, 2002; Vol. 2, p 749.
(8) Becerra, R.; Boganov, S. E.; Egorov, M. P.; Nefedov, O. M.; Walsh, R. *Chem. Phys. Lett.* **1996**, *260*, 433.
(9) Becerra, R.; Boganov, S. E.; Egorov, M. P.; Faustov, V. I.; Promyslov, V. M.; Nefedov, O. M.; Walsh, R. *Phys. Chem. Chem. Phys.* **2002**, *4*, 5079.
(10) Becerra, R.; Walsh, R. *J. Organomet. Chem.* **2001**, *636*, 49.
(11) Becerra, R.; Walsh, R. *Phys. Chem. Chem. Phys.* **2002**, *4*, 6001.
(12) Alexander, U. N.; King, K. D.; Lawrance, W. D. *Chem. Phys. Lett.* **2000**, *319*, 529.
(13) Becerra, R.; Boganov, S. E.; Egorov, M. P.; Faustov, V. I.; Krylova, I. V.; Nefedov, O. M.; Promyslov, V. M.; Walsh, R. *Phys. Chem. Chem. Phys.* **2004**, *6*, 3370.
(14) Becerra, R.; Walsh, R. *Phys. Chem. Chem. Phys.* **2009**, *11*, 3539.
(15) Becerra, R.; Walsh, R. *Phys. Chem. Chem. Phys.* **1999**, *1*, 5301.
(16) Becerra, R.; Boganov, S. E.; Egorov, M. P.; Faustov, V. I.; Nefedov, O. M.; Walsh, R. *Phys. Chem. Chem. Phys.* **2001**, *3*, 184.
(17) Becerra, R.; Boganov, S. E.; Egorov, M. P.; Faustov, V. I.; Nefedov, O. M.; Walsh, R. *J. Am. Chem. Soc.* **1998**, *120*, 12657.
(18) Alexander, U. N.; Trout, N. A.; King, K. D.; Lawrance, W. D. *Chem. Phys. Lett.* **1999**, *299*, 291.
(19) Becerra, R.; Egorov, M. P.; Krylova, I. V.; Nefedov, O. M.; Walsh, R. *Chem. Phys. Lett.* **2002**, *351*, 47.
(20) Becerra, R.; Boganov, S. E.; Egorov, M. P.; Faustov, V. I.; Krylova, I. V.; Nefedov, O. M.; Promyslov, V. M.; Walsh, R. *Phys. Chem. Chem. Phys.* **2007**, *9*, 4395.
(21) Alexander, U. N.; King, K. D.; Lawrance, W. D. *Phys. Chem. Chem. Phys.* **2003**, *5*, 1557.
(22) (a) Thimer, K. C.; Al-Rafia, S. M. I.; Ferguson, M. J.; McDonald, R.; Rivard, E. *Chem. Commun.* **2009**, 7119. (b) Al-Rafia, S. M. I.; Malcolm, A. C.; Liew, S. K.; Ferguson, M. J.; Rivard, E. *J. Am. Chem. Soc.* **2011**, *133*, 777.
(23) (a) Rupar, P. A.; Jennings, M. C.; Ragogna, P. J.; Baines, K. M. *Organometallics* **2007**, *26*, 4109. (b) Ghadwal, R. S.; Roesky, H. W.; Merkel, S.; Stalke, D. *Chem. -Eur. J.* **2010**, *16*, 85. (c) Li, J.; Merkel, S.; Henn, J.; Meindl, K.; Döring, A.; Roesky, H. W.; Ghadwal, R. S.; Stalke, D. *Inorg. Chem.* **2010**, *49*, 775.
(24) Goldberg, D. E.; Hitchcock, P. B.; Lappert, M. F.; Thomas, K. M.; Thorne, A. J.; Fjeldberg, T.; Haaland, A.; Schilling, B. E. R. *J. Chem. Soc., Dalton Trans.* **1986**, *1986*, 2387.
(25) Grev, R. S.; Schaefer, H. F., III; Baines, K. M. *J. Am. Chem. Soc.* **1990**, *112*, 9458.
(26) Ricca, A.; Bauschlicher, C. W. *J. Phys. Chem. A* **1999**, *103*, 11121.
(27) Chen, W. C.; Su, M. D.; Chu, S. Y. *Organometallics* **2001**, *20*, 564.
(28) Becerra, R.; Harrington, C. R.; Gaspar, P. P.; Leigh, W. J.; Vargas-Baca, I.; Walsh, R.; Zhou, D. *J. Am. Chem. Soc.* **2005**, *127*, 17469.
(29) Trinquier, G. *J. Am. Chem. Soc.* **1990**, *112*, 2130.
(30) Grev, R. S.; Schaefer, H. F., III *Organometallics* **1992**, *11*, 3489.
(31) Li, Q.-S.; Lu, R.-H.; Xie, Y.; Schaefer, H. F. I. *J. Comput. Chem.* **2002**, *23*, 1642.
(32) Carrier, W.; Zheng, W.; Osamura, Y.; Kaiser, R. I. *Chem. Phys.* **2006**, *330*, 275.
(33) Wang, X.; Andrews, L.; Kushto, G. P. *J. Phys. Chem. A* **2002**, *106*, 5809.
(34) Leigh, W. J.; Harrington, C. R.; Vargas-Baca, I. *J. Am. Chem. Soc.* **2004**, *126*, 16105.
(35) Leigh, W. J.; Lollmahomed, F.; Harrington, C. R. *Organometallics* **2006**, *25*, 2055.
(36) Leigh, W. J.; Lollmahomed, F.; Harrington, C. R.; McDonald, J. M. *Organometallics* **2006**, *25*, 5424.
(37) Lollmahomed, F.; Huck, L. A.; Harrington, C. R.; Chitnis, S. S.; Leigh, W. J. *Organometallics* **2009**, *28*, 1484.
(38) Lollmahomed, F.; Leigh, W. J. *Organometallics* **2009**, *28*, 3239.
(39) Leigh, W. J.; Harrington, C. R. *J. Am. Chem. Soc.* **2005**, *127*, 5084.
(40) Huck, L. A.; Leigh, W. J. *Organometallics* **2007**, *26*, 1339.
(41) Huck, L. A.; Leigh, W. J. *Organometallics* **2009**, *28*, 6777.
(42) Leigh, W. J.; Dumbrava, I. G.; Lollmahomed, F. *Can. J. Chem.* **2006**, *84*, 934.
(43) Becerra, R.; Boganov, S. E.; Egorov, M. P.; Lee, V. Y.; Nefedov, O. M.; Walsh, R. *Chem. Phys. Lett.* **1996**, *250*, 111.
(44) Saito, K.; Obi, K. *Chem. Phys.* **1994**, *187*, 381.
(45) Becerra, R.; Boganov, S. E.; Egorov, M. P.; Faustov, V. I.; Nefedov, O. M.; Walsh, R. *Can. J. Chem.* **2000**, *78*, 1428.
(46) Becerra, R.; Boganov, S. E.; Egorov, M. P.; Krylova, I. V.; Nefedov, O. M.; Walsh, R. *J. Phys. Chem. A* **2007**, *111*, 1434.
(47) Perdew, J. P.; Burke, K. *Int. J. Quantum Chem.* **1996**, *57*, 309.
(48) Gibbon, G. A.; Rousseau, Y.; Van Dyke, C. H.; Mains, G. J. *Inorg. Chem.* **1966**, *5*, 114.
(49) Angus, P. C.; Stobart, S. R. *J. Chem. Soc., Dalton Trans.* **1975**, *1975*, 2342.
(50) Farkas, A. *Orthohydrogen, Parahydrogen and Heavy Hydrogen*; Cambridge University Press: London, 1935.
(51) Benoit, H.; Piejus, P. *C. R. Acad. Sci. Ser. B* **1967**, *265B*, 101.
(52) In addition to the resonances due to HD and **8**-*d*, the spectrum of the **4**/AcOD photolysate also showed evidence for the formation of small amounts of H_2 and all-protiated **8**, in similar relative yields to what was obtained in the **4**/AcOH photolysis. We thus conclude that the formation of H_2 in the **4**/AcOD experiment is due to the presence of small amounts of AcOH in the mixture and not to unimolecular elimination of H_2 from **4**.
(53) Massol, M.; Satge, J.; Riviere, P.; Barrau, J. *J. Organomet. Chem.* **1970**, *22*, 599.
(54) Gibbon, G. A.; Wang, J. T.; Van Dyke, C. H. *Inorg. Chem.* **1967**, *6*, 1989.
(55) Heaven, M. W.; Metha, G. F.; Buntine, M. A. *J. Phys. Chem. A* **2001**, *105*, 1185.
(56) Heaven, M. W.; Metha, G. F.; Buntine, M. A. *Aust. J. Chem.* **2001**, *54*, 185.
(57) Moiseev, A. G.; Leigh, W. J. *Organometallics* **2007**, *26*, 6268.
(58) Moiseev, A. G.; Coulais, E.; Leigh, W. J. *Chem.—Eur. J.* **2009**, *15*, 8485.
(59) Mochida, K.; Kayamori, T.; Wakasa, M.; Hayashi, H.; Egorov, M. P. *Organometallics* **2000**, *19*, 3379.
(60) Nag, M.; Gaspar, P. P. *Organometallics* **2009**, *28*, 5612.
(61) Neumann, W. P.; Sakurai, H.; Billeb, G.; Brauer, H.; Kocher, J.; Viebahn, S. *Angew. Chem., Int. Ed. Engl.* **1989**, *28*, 1028.
(62) Sakai, S. *Int. J. Quantum Chem.* **1998**, *70*, 291.
(63) Su, M. D.; Chu, S. Y. *J. Am. Chem. Soc.* **1999**, *121*, 11478.
(64) Birukov, A. A.; Faustov, V. I.; Egorov, M. P.; Nefedov, O. M. *Russ. Chem. Bull. Int. Ed.* **2005**, *54*, 2003.
(65) Joo, H.; Kraka, E.; Quapp, W.; Cremer, D. *Mol. Phys.* **2007**, *105*, 2697.
(66) Summerscales, O. T.; Jimenez-Halla, J. O. C.; Merino, G.; Power, P. P. *J. Am. Chem. Soc.* **2011**, *133*, 180.
(67) (a) Grimme, S. *J. Chem. Phys.* **2006**, *124*, 034108. (b) Grimme, S.; Neese, F. *J. Chem. Phys.* **2007**, *127*, 154116.
(68) Adamo, C.; Barone, V. *J. Chem. Phys.* **1999**, *110*, 6158.
(69) Curtiss, L. A.; Redfern, P. C.; Raghavachari, K. *J. Chem. Phys.* **2007**, *126*, 084108.
(70) Becerra, R.; Harrington, C. R.; Leigh, W. J.; Kefala, L. A.; Walsh, R. *Organometallics* **2006**, *25*, 4439.
(71) Neumann, W. P. *Chem. Rev.* **1991**, *91*, 311.